Journal of Statistical Physics, Vol. 36, Nos. 3/4, 1984

The Kinetic Boundary Layer for the Klein–Kramers Equation; A New Numerical Approach

Jonathan V. Selinger[1,2] and U. M. Titulaer[1]

Received October 27, 1983; revision received March 1, 1984

We explore a numerical technique for determining the structure of the kinetic boundary layer of the Klein–Kramers equation for noninteracting Brownian particles in a fluid near a wall that absorbs the Brownian particles. The equation is of interest in the theory of diffusion-controlled reactions and of the coagulation of colloidal suspensions. By numerical simulation of the Langevin equation equivalent to the Klein–Kramers equation we amass statistics of the velocities at the first return to the wall and of the return times for particles injected into the fluid at the wall with given velocities. The data can be used to construct the solutions of the standard problems at an absorbing wall, the Milne and the albedo problem. We confirm and extend earlier results by Burschka and Titulaer, obtained by a variational method vexed by the slow convergence of the underlying eigenfunction expansion. We briefly discuss some further boundary layer problems that can be attacked by exploiting the results reported here.

KEY WORDS: Boundary layer; Brownian motion; diffusion-controlled reactions; Milne problem; albedo problem; numerical simulation.

1. INTRODUCTION AND SURVEY

Kinetic boundary layers occur in systems described by kinetic equations when one imposes boundary conditions that cannot be satisfied by a distribution function of local equilibrium type. In such layers the Chapman–Enskog solution procedure breaks down: to satisfy the boundary conditions the Chapman–Enskog solution must be supplemented by a boundary layer solution, concentrated in a region near the wall with a thickness of the order of the mean free path. Knowledge of this boundary

[1] Institut für Theoretische Physik A, Rheinisch-Westfälische Technische Hochschule, Templergraben 55, 5100 Aachen, Federal Republic of Germany.

[2] Present address: Department of Physics, Harvard University, Cambridge, Massachusetts 02138.

0022-4715/84/0800-0293$03.50/0

822/36/3-4-1

layer solution is necessary to determine the boundary conditions to be imposed on the hydrodynamic equations derived by means of the Chapman–Enskog method, in particular the so-called slip or accommodation coefficients.[1] An example of such a slip coefficient is the Milne extrapolation length near an absorbing or partially absorbing wall.[2]

The explicit construction of a boundary layer solution has thus far been achieved only for plane walls and for very simple kinetic equations, in which the collision operator has but a single nonzero eigenvalue. Examples are the radiative transfer equation for grey matter[2] (or the mathematically identical one-speed neutron transport equation) and the BGK model for the linearized Boltzmann equation.[1] In one of its variants this exact solution proceeds in two steps. First one constructs a set of fundamental boundary layer solutions. Subsequently, one finds a particular linear combination of them that satisfies the boundary condition; this is accomplished by means of a so-called half-range expansion formula.[3]

The same solution strategy can be followed for more general kinetic equations. The required modifications of the formalism for the linearized Boltzmann equation can be found in a paper by Waldmann and Vestner.[4] However, in general neither the fundamental boundary layer solutions nor the half-range expansion formula are known explicitly. Hence one must rely on approximate procedures, whose quality is hard to asses.

A case of intermediate tractability is provided by the Klein–Kramers equation[5] for positions and velocities of an assembly of noninteracting Brownian particles in a fluid. Its solutions exhibit a kinetic boundary layer near a completely or partially absorbing wall.[6] Such solutions are of interest for the description of diffusion-controlled reactions of large molecules in a fluid,[7] or of coagulation in colloidal suspensions.[8] For this case the fundamental boundary layer solutions at a plane wall in the absence of any external forces on the Brownian particles were found by Pagani,[9] and their analogs for a uniform external force by Burschka and Titulaer.[10] Moreover, the existence of a half-range expansion formula was recently proved rigorously by Beals and Protopopescu[11]; the proof can be extended to a large class of differential equations of Sturm–Liouville type.[27] Similar results for a class of problems including certain integrodifferential equations similar to the linearized Boltzmann equation were proved by Greenberg and van der Mee.[28]

The existence proof in Ref. 11 does not provide a recipe to construct the solution via a half-range expansion formula. One way to construct the solution, carried out by Burschka and Titulaer[12,10] and justified a posteriori by the results of Ref. 11, is to approximate it by finite sums of fundamental boundary layer solutions, optimized via a variational principle. However, since the expansion of the desired solution in terms of the fundamental ones

converges very slowly, this method requires extensive numerical computations. Even the best linear combination of 140 fundamental solutions does not satisfy the boundary conditions very well, but some physical quantities of interest, such as the Milne extrapolation length, can be predicted with confidence using an empirical extrapolation procedure. The reasons for the slow convergence can be understood from the asymptotic behavior of the Pagani solutions.[13] Replacing the variational procedure by a moment matching method due to Marshak,[14] as proposed by Razi Naqvi *et al.*, appears to improve the initial rate of convergence,[3] but the method has the same basic drawback: one tries to approximate a nondifferentiable function by a linear combination of analytic basis functions. Replacing the exact Pagani solutions by approximate ones, as done in Ref. 15 and in earlier work by Harris,[17] offers little hope for fundamental improvement.

In the present work we do not attempt to base our treatment on an explicit expansion in terms of the Pagani solutions. Instead we exploit a theorem, discussed more fully in the next section, that reduces the expansion to quadratures once an auxiliary problem, the albedo problem, has been solved. In the albedo problem one considers a particle injected into the system at the wall with a given velocity, and asks for the probability distribution of its velocity when it returns to the wall for the first time. (The particle is sure to return when the wall is plane; the problem is a variant of the gambler's ruin problem.[18]) The solution of the albedo problem is found via a numerical simulation of the Klein–Kramers equation, or rather of the equivalent Langevin equation. There is one complication: since the mean value of the time of first return is infinite, a straightforward simulation is impossible; we find that, for a typical distribution of injection velocities, about 60% of the particles have returned after 15 relaxation times. However, their velocity distribution as a function of the return time rapidly approaches a limit, and it appears safe to assume that the particles returning after 15 relaxation times will exhibit this same asymptotic velocity distribution. This conjecture is supported by an approximate analytical treatment. Once we accept the conjecture on the velocity distribution of the late returners, the solution of the albedo problem is complete.

The remainder of this paper is organized as follows: in Section 2 we discuss in more detail the Pagani solutions and the relation between the half-range expansion formula and the solution of the albedo problem. In Section 3 we discuss our simulation procedure and the evidence for the conjecture on the velocity spectrum for the late returners. In Section 4 we discuss the stationary solution of the Klein–Kramers equation with a plane absorbing

[3] For similar observations concerning the Boltzmann equation see Ref. 16.

wall, as constructed from the results of our simulation. The results are compared with those of earlier treatments. Section 5 is devoted to a more detailed discussion of our numerical solution of the albedo problem. In particular we provide a convenient parametrization of the albedo kernel. This kernel expresses the velocity distribution of the Brownian particles at their first return in terms of their velocity distribution at injection. In Section 6 we show how knowledge of the albedo kernel enables one to solve problems with a partially absorbing wall. We give explicit results for the simplest such case, where particles that are not absorbed are reinjected with a velocity distribution corresponding to thermal equilibrium at the temperature of the fluid. Section 7 contains a few concluding remarks.

2. BASIC EQUATIONS AND THEOREMS

The Klein–Kramers equation for the probability distribution of position $\mathbf{x}$ and velocity $\mathbf{u}$ of a Brownian particle in a fluid reads

$$\frac{\partial P(\mathbf{u}, \mathbf{x}, t)}{\partial t} = \left[-\mathbf{u} \cdot \frac{\partial}{\partial \mathbf{x}} + \gamma \left(\frac{1}{m\beta} \frac{\partial}{\partial \mathbf{u}} \cdot \frac{\partial}{\partial \mathbf{u}} + \frac{\partial}{\partial \mathbf{u}} \cdot \mathbf{u} \right) \right] P(\mathbf{u}, \mathbf{x}, t) \quad (2.1)$$

where γ is the friction constant, m is the mass of the particle, and β equals $(kT)^{-1}$ with T the temperature of the fluid. In the remainder of this paper we shall use units such that $\gamma = m\beta = 1$. This means that times are measured in units γ^{-1} and lengths in units of $l = \gamma^{-1}(m\beta)^{-1/2}$, the velocity persistence length[19] that plays the role of a mean free path in the kinetic equation (2.1). Furthermore, we are interested only in stationary solutions with full translational symmetry in the y and z direction. Such solutions must have the form

$$P(\mathbf{u}, \mathbf{x}, t) = (2\pi)^{-1} \exp[-\tfrac{1}{2}(u_y^2 + u_z^2)]\, P(u_x, x) \quad (2.2)$$

with $P(u_x, x)$ a solution of

$$u \frac{\partial}{\partial x} P(u, x) = \left[\frac{\partial^2}{\partial u^2} + \frac{\partial}{\partial u} u \right] P(u, x) \quad (2.3)$$

where we replaced the variable u_x by u.

The reduced Klein–Kramers equation (2.3) has two independent solutions of Chapman–Enskog type, for which the density $n(x) = \int P(u, x)\, du$ obeys the diffusion equation $(\partial^2/\partial x^2)\, n(x) = 0$. These are the equilibrium solution

$$\psi_0(u, x) = \phi_0(u) = (2\pi)^{-1/2} \exp[-\tfrac{1}{2}u^2] \quad (2.4)$$

and a current-carrying solution:

$$\psi_0'(u, x) = (xu^{-1} - 1)\,\phi_0'(u) \tag{2.5a}$$

with

$$\phi_0'(u) = (2\pi)^{-1/2} u \exp[-\tfrac{1}{2}u^2] \tag{2.5b}$$

In addition, (2.3) has the fundamental boundary layer solutions found by Pagani[9]

$$\psi_{\pm n}(u, x) = \exp[\mp x n^{1/2}]\,\phi_{\pm n}(u), \qquad n = 1, 2, 3,... \tag{2.6a}$$

with

$$\phi_{\pm n}(u) = (n!)^{-1/2}(8\pi n)^{-1/4}(2e)^{-n/2} \exp[-\tfrac{1}{2}(u \mp n^{1/2})^2] \times H_n[2^{-1/2}(u \mp 2n^{1/2})] \tag{2.6b}$$

and $H_n(\xi)$ the nth Hermite polynomial.

The set of functions $\{\phi_0(u), \phi_0'(u), \phi_{\pm n}(u)\}$ is orthogonal and complete on $-\infty < u < \infty$ with respect to the indefinite scalar product

$$\langle f, g\rangle = \int_{-\infty}^{+\infty} du\, u \exp[\tfrac{1}{2}u^2]\, f(u)\, g(u) \tag{2.7}$$

The orthogonality relations are[9]

$$\begin{gathered}\langle \phi_{+n}, \phi_{+m}\rangle = \delta_{nm}, \qquad \langle \phi_{-n}, \phi_{-m}\rangle = -\delta_{nm} \\ \langle \phi_{+n}, \phi_{-m}\rangle = \langle \phi_{\pm n}, \phi_0\rangle = \langle \phi_{\pm n}, \phi_0'\rangle = 0 \\ \langle \phi_0, \phi_0'\rangle = (2\pi)^{-1/2}, \qquad \langle \phi_0, \phi_0\rangle = \langle \phi_0', \phi_0'\rangle = 0\end{gathered} \tag{2.8}$$

Any function $f(u)$ such that

$$\int du\, |u| \exp[\tfrac{1}{2}u^2]\, f^2(u) < \infty \tag{2.9a}$$

can be expanded according to[9,11]

$$f(u) = d_0\phi_0(u) + d_0'\phi_0'(u) + \sum_{n=1}^{\infty} [d_{-n}\phi_{-n}(u) + d_{+n}\phi_{+n}(u)] \tag{2.9b}$$

with

$$\begin{gathered}d_{+n} = \langle \phi_{+n}, f\rangle, \qquad d_{-n} = -\langle \phi_{-n}, f\rangle \\ d_0 = (2\pi)^{1/2}\langle \phi_0', f\rangle, \qquad d_0' = (2\pi)^{1/2}\langle \phi_0, f\rangle\end{gathered} \tag{2.9c}$$

The completeness relation (2.9b) allows one to construct a solution $P(u, x)$ of (2.3) with prescribed values $P(u, 0) = f(u)$: one simply replaces the $\phi(u)$ in (2.9b) by the corresponding $\psi(u, x)$. However, this solution will in general grow exponentially in both x directions, and it is not likely to be of physical interest. In most half-space problems one must satisfy boundary conditions of a different kind: only the density of the particles with $u > 0$ is prescribed at the boundary (assuming the medium is to the right of $x = 0$), but we accept only solutions without parts that grow exponentially for $x \to \infty$. Physically one expects[19] that for $x \gg 1$ the solution approaches one of Chapman–Enskog type, i.e., a linear combination of ψ_0 and ψ_0'. A typical boundary layer problem is the following.

The Albedo Problem[2]. Find a solution of the form

$$P^f(u, x) = d_0^f \phi_0(u) + \sum_{n=1}^{\infty} d_{+n}^f \psi_{+n}(u, x), \qquad x \geqslant 0 \tag{2.10a}$$

such that

$$P^f(u, 0) = f_+(u) \qquad \text{for} \quad u > 0 \tag{2.10b}$$

This corresponds to the situation that $uf_+(u)\,du$ particles with velocities in du around u are injected into the fluid at $x = 0$ per unit time (leading to a *particle density* $f_+(u)$ for $u > 0$), and leave the fluid at their first return to the plane $x = 0$. The velocity distribution of the emerging particles is then given by

$$uf_-(u) \equiv uP^f(-u, 0) \tag{2.11}$$

A sufficient condition for the unique solvability of the albedo problem is the *half-range completeness property*: $f_+(u)$ possesses a unique expansion of the form

$$f_+(u) = d_0^f \phi_0(u) + \sum_{n=1}^{\infty} d_{+n}^f \phi_{+n}(u) \qquad \text{for} \quad u > 0 \tag{2.12}$$

The existence and uniqueness of such an expansion was proved by Beals and Protopopescu[11] for $f_+(u)$ that obey (2.9a). An alternative formulation of this result is: each $f_+(u)$ has a unique continuation $f_-(-u)$ such that $f_+(u) + f_-(-u)$ lies in the subspace spanned by $\phi_0(u)$ and the $\phi_{+n}(u)$ with $n = 1, 2, \ldots$. Owing to the linearity of the albedo problem, the functions $f_+(u)$ and $f_-(u)$ must be linearly related; this relation can be expressed by means of the *albedo kernel* $A(u \mid u')$ defined by

$$uf_-(u) = \int_0^{\infty} du'\, A(u \mid u')\, u' f_+(u') \tag{2.13}$$

The albedo kernel expresses the probability that a particle injected into the fluid with velocity u' will leave it with velocity $-u$. Once $P^f(u, 0) = f_+(u) + f_-(-u)$ is known, the full solution $P^f(u, x)$ can be constructed via the full-range completeness relation (2.9b), as discussed earlier.

A second important boundary problem is the *Milne problem*: construct a solution of (2.3) of the form

$$P^M(u, x) = \psi_0'(u, x) + d_0^M \phi_0(u) + \sum_{n=1}^{\infty} d_{+n}^M \psi_{+n}(u, x), \qquad x \geqslant 0 \quad (2.14a)$$

such that

$$P^M(u, 0) = 0 \qquad \text{for} \quad u > 0 \quad (2.14b)$$

This describes the situation that a constant current of particles, of value unity, flows from $+\infty$ toward a wall at $x = 0$ that absorbs all Brownian particles impinging on it. The solution follows from that of the albedo problem:

$$\begin{aligned} P^M(u, 0) &= \phi_0'(u) + |u|^{-1} \int_0^{\infty} du' A(u \mid u')\, u' \phi_0'(u') \qquad \text{for} \quad u < 0 \\ &= 0 \qquad\qquad\qquad\qquad\qquad\qquad\qquad\quad \text{for} \quad u > 0 \end{aligned} \quad (2.15)$$

The expansion coefficients d_0^M and d_{+n}^M then follow via (2.9). The coefficient d_0^M plays a special role; from (2.14a), (2.4) and (2.5) follows:

$$n^M(x) \equiv \int du P^M(u, x) \approx x + (2\pi)^{1/2} d_0^M \equiv x + x_M \qquad \text{for} \quad x \gg 1 \quad (2.16)$$

This means that the solution of the diffusion equation that $n^M(x)$ approaches for large x does not extrapolate to zero at $x = 0$, but at $x = -x_M$. The quantity x_M is the Milne extrapolation length mentioned in the Introduction. Using (2.8), (2.9), and (2.14) we find

$$x_M = \int_{-\infty}^{0} du\, u^2 P^M(u, 0) \quad (2.17)$$

This simple expression for x_M emerged only since we normalized $P^M(u, x)$ to have unit current; in general one has[12]

$$x_M = \int_{-\infty}^{\infty} du\, u^2 P(u, 0) \Big/ \int_{-\infty}^{\infty} du\, u P(u, 0) \quad (2.18)$$

We conclude this section by introducing a set of polynomials that will prove useful in representing numerically determined functions on the half line $0 \leqslant u < \infty$ in the form

$$f(u) \simeq q(u) \exp[-\tfrac{1}{2}u^2] \tag{2.19}$$

with $q(u)$ a polynomial. One could use either the odd or the even Hermite polynomials of argument $2^{-1/2}u$, but these are tailored to functions with $f(0) = 0$ or $f'(0) = 0$, respectively; they provide poor approximations when neither condition is fulfilled. Therefore we constructed by means of the Gram–Schmidt procedure[20] a set of polynomials $q_n(u)$ such that

$$\int_0^\infty du \exp[-\tfrac{1}{2}u^2]\, q_n(u)\, q_m(u) = \delta_{nm} \tag{2.20}$$

The first five of these polynomials are given in Table I. They have the property that

$$f^N(u) = \exp[-\tfrac{1}{2}u^2] \sum_{n=1}^{N} s_n q_n(u) \tag{2.21a}$$

with

$$s_n = \int_0^\infty du q_n(u) f(u) \tag{2.21b}$$

is the best approximation of type (2.19) to $f(u)$ using a polynomial of degree N, when the error is measured by the weighted integral

$$\Delta_N = \int_0^\infty du \exp[\tfrac{1}{2}u^2]\, |f(u) - f^N(u)|^2 \tag{2.21c}$$

The weight function in (2.21c), the inverse of the Maxwell equilibrium distribution, will appear to be a natural one in the applications of the fitting procedure in Sections 4 and 5, for reasons more fully explained in Section 5.

Table I. The First Five Polynomials $q_n(u)$, Constructed to be Orthonormal with Respect to the Weight $\exp[-(1/2)u^2]$.

	1	u	u^2	u^3	u^4
$q_0(u)$	0.8932				
$q_1(u)$	−1.1823	1.4818			
$q_2(u)$	1.3486	−3.9379	1.7935		
$q_3(u)$	−1.4684	7.2500	−7.1641	1.7846	
$q_4(u)$	1.5642	−11.3526	18.0474	−9.5113	1.5414

3. THE SIMULATION PROCEDURE

The calculational basis for the results reported in this paper is the determination of the albedo kernel $A(u \mid u')$, defined in (2.13), via a numerical simulation. The one-dimensional Klein–Kramers equation is equivalent to the Langevin equations[21]

$$\dot{x} = u, \qquad \dot{u} = -\gamma u + \xi(t) \tag{3.1a}$$

with $\xi(t)$ a Gaussian stochastic process obeying

$$\langle \xi(t) \rangle = 0, \qquad \langle \xi(t)\, \xi(t') \rangle = 2\gamma(m\beta)^{-1}\, \delta(t - t') \tag{3.1b}$$

Numerical solution of this equation requires a discretizaton; as such we choose, in units such that $\gamma = m\beta = 1$,

$$x(t + \tau) = x(t) + \tau u(t) \tag{3.2a}$$

$$u(t + \tau) = (1 - \tau)\, u(t) + \xi_\tau \tag{3.2b}$$

with ξ_τ a Gaussian random variable such that

$$\langle \xi_\tau \rangle = 0, \qquad \langle \xi_\tau^2 \rangle = 2\tau - \tau^2 \tag{3.2c}$$

The choice (3.2c) ensures that $\langle u^2(t) \rangle$ approaches the correct value unity when (3.2b) is iterated.

To generate data for the determination of $A(u \mid u')$ we use the initial values $x(0) = 0$ and $u(0) = u'$ and iterate (3.2a, b) until $x(n\tau) < 0$, or until n reaches a predetermined maximum value, for which we took $n\tau = 15$. If $x(n\tau) < 0$ we register a returning particle at $t_R = n\tau$ with velocity $u_R = u[(n-1)\tau]$. This ensures a negative return velocity; any attempt to correct for velocity changes in the final time interval would lead to some positive "return velocities," which would be physically unacceptable. [In view of this, refinements of the simple linearization (3.2a, b) were rejected as of doubtful consistency.] Repeating this procedure for different realizations of the stochastic process ξ_τ yields a distribution of return times and return velocities for either a given fixed initial velocity or for a given distribution $j(u')$ of initial velocities. The distribution so obtained will be denoted by $N_\tau(u_R, t_R \mid u')$ or, for a distribution of initial velocities, by

$$N_\tau(u_R, t_R \mid j(u')) = \int du'\, N_\tau(u_R, t_R \mid u')\, j(u') \tag{3.3}$$

To guide the choice of the time step τ in the main simulation we performed trial simulations of 3000 particles each for velocities distributed

uniformly in the intervals $0 < u' < 0.5$, $1 < u' < 1.5$ and $2 < u' < 2.5$, and for time steps $\tau = 0.05$, 0.02, 0.01, and 0.005. The results for several moments of the form

$$\int_0^{15} dt_R \int_0^{\infty} du_R u_R^{\alpha} N_{\tau}(u_R, t_R \mid j(u'))$$

are given in Table II, together with their statistical error. We notice hardly any trend with τ for the particles injected with the higher velocities. For slowly injected particles there is a clear trend, reflecting the fact that very low *return* velocities become more frequent as the time step gets smaller; this mainly influences the data for low injection velocities, since slowly injected particles are more likely to return slowly. Discretization errors are expected to be most serious for slowly returning particles: a "soft landing" becomes increasingly less likely as the "power bursts" become larger in the mean and spaced at larger intervals. For our main simulation we chose $\tau = 0.01$. This still involves a small systematic error for low return velocities, but allows us to obtain good statistics overall. The index τ will henceforth be omitted.

For our main simulation we followed 10^5 particles with an initial distribution $j_c(u') \sim u'\phi_0'(u')\,\Theta(u')$; this distribution was chosen to generate accurate data for the solution (2.15) of the Milne problem. However, we kept track of the initial velocities u' of each of the particles, in order to obtain results for the albedo kernel itself as well. To obtain $A(u_R \mid u')$ we must

Table II. The Moments $\langle u \rangle$ and $\langle u^2 \rangle$ of the Distribution $f_-(u)$ Corresponding to Particles Injected with Uniform Velocity Distribution in Three Velocity Intervals, and Returning before $t = 15$, as Determined from Simulations with 3000 Particles Each Using four Different Discretization Intervals τ

	τ	0.05	0.02	0.01	0.005	$(\sigma)^a$
$0 < u' < 0.5$	$\langle u \rangle$	0.355	0.322	0.314	0.258	(7)
	$\langle u^2 \rangle$	0.268	0.236	0.225	0.176	(12)
$1 < u' < 1.5$	$\langle u \rangle$	0.767	0.715	0.746	0.721	(11)
	$\langle u^2 \rangle$	0.844	0.780	0.805	0.778	(24)
$2 < u' < 2.5$	$\langle u \rangle$	0.866	0.892	0.893	0.893	(13)
	$\langle u^2 \rangle$	1.088	1.103	1.107	1.101	(30)

[a] The "errors" shown in this column (in units of the last digit given) are calculated from $(N-1)\sigma^2 = \langle a^2 \rangle - \langle a \rangle^2$; owing to the skewness of the distribution, especially at high u', this overestimates the real statistical error.

integrate $N(u_R, t_R \mid u')$ over all t_R, not just up to $t_R = 15$; of the 10^5 particles, only 59 997 have returned before this time. However, the moments defined as

$$\langle\langle u_R^\alpha(t_R)\rangle\rangle \equiv \int du_R\, u_R^\alpha N(u_R, t_R \mid j_c) \Big/ \int du_R\, N(u_R, t_R \mid j_c)$$

approach a limit for large t_R, as in shown for $\langle\langle u_R(t_R)\rangle\rangle$ in Fig. 1. We attempted to fit the simulation results for $\langle\langle u_R^\alpha(t_R)\rangle\rangle$, $\alpha = \pm 1$, sampled in intervals $\Delta t_R = 0.5$ with trial functions of the type

$$\langle\langle u_R^\alpha(t_R)\rangle\rangle = a_\alpha + b_\alpha \exp[-c_\alpha t_R] \tag{3.4}$$

and

$$\langle\langle u_R^\alpha(t_R)\rangle\rangle = p_\alpha + q_\alpha t_R^{s_\alpha} \tag{3.5}$$

for the interval $6 < t_R \leqslant 15$. The fits of type (3.4) were invariably better and the best values for c were around 0.4 for $\alpha = 1$ and $\alpha = -1$. For $10 < t_R \leqslant 15$ no significant t_R dependence was detected by our fitting procedure.

These results imply that the velocity spectrum for $t_R > 15$ will not be too different from the one for $t_0 < t_R \leqslant 15$ with large enough t_0; t_0 should be chosen such that the remaining systematic error, as estimated from (3.4), is small compared to the statistical error, which increases with increasing t_0.

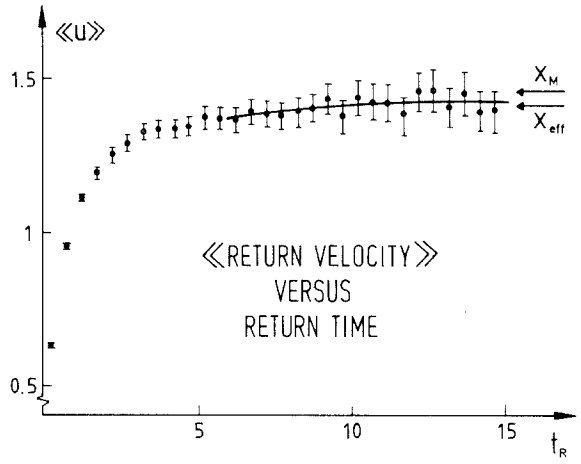

Fig. 1. The average return velocity as a function of return time for a sample of 10^5 injected particles with distribution $u'\phi_0'(u')$. The error bars are statistical uncertainties calculated as if for a normal distribution. The curve is the best fit of type (3.4). At the right we indicated the limit x_M for high t_R and the average x_{eff} over $8 < t_R \leqslant 15$.

This criterion yields a value of t_0 between 6 and 10; we chose $t_0 = 8$ for our calculations. This means that we approximate $A(u \mid u')$ by

$$A(u \mid u') = \frac{1}{N(u')} \left[\int_0^8 dt_R \, N(u, t_R \mid u') + \frac{\mathcal{N}_>(u, 8 \mid u')}{\mathcal{N}_>(u, 8 \mid u') - \mathcal{N}_>(u, 15 \mid u')} \int_8^{15} dt_R \, N(u, t_R \mid u') \right] \quad (3.6a)$$

with

$$\mathcal{N}_>(u, t \mid u') = N(u') - \int_0^t dt_R \, N(u, t_R \mid u') \quad (3.6b)$$

and $N(u')$ the number of particles in the simulation with initial velocity u'. In practice, the $\mathcal{N}_>$ are of course determined by averaging over sample intervals of u and u'; we used a sampling interval of 0.05. To minimize the influence of the sampling errors we did not use the corrected $A(u \mid u')$ for determining the solution (2.15) of the Milne problem, but performed instead the analogous correction on the integral over $A(u \mid u')$ appearing in (2.15).

As a check we show in Fig. 2 the statistics of return velocities corresponding to an initial velocity distribution

$$j_0(u') \sim u' \exp[-\tfrac{1}{2}u'^2]$$

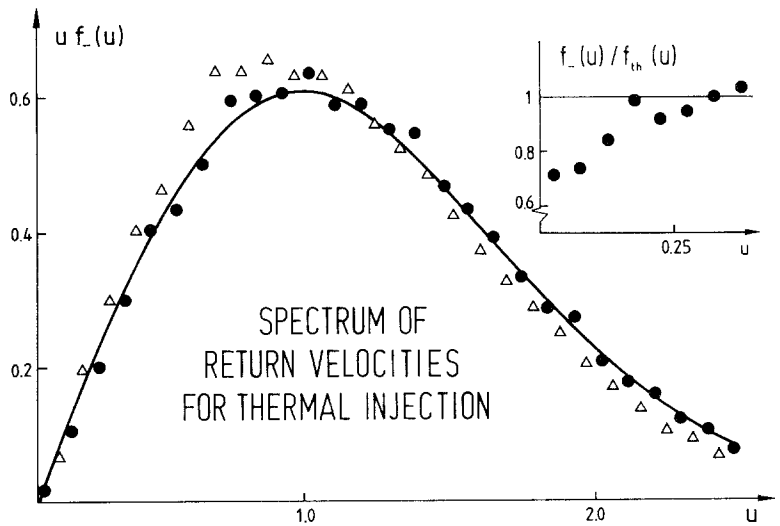

Fig. 2. The return velocity spectrum for an equilibrium distribution $u'\phi_0(u')$ of injection velocities. The curve is the theoretical spectrum; the spectrum measured for $0 < t_R \leqslant 15$ (after rescaling) is indicated by △; the spectrum after correction for the late returners by ●. The insert shows the ratio of the corrected and the theoretical spectrum for very low return velocities; the shortfall is ascribed to discretization errors.

This corresponds to a thermal equilibrium distribution for the injected particles, and the return velocities should have the same equilibrium distribution, shown as a full curve in the figure. The "experimental" distributions are the spectrum of return velocities for $t_R \leqslant 15$, rescaled to have the same area, and the result calculated with the $A(u \mid u')$ as determined by (3.6). The discrepancy between the latter and the theoretical curve is barely larger than the statistical uncertainly in the points calculated with the corrected $A(u \mid u')$, determined in a way explained more fully in Section 4. The discrepancy is, moreover, almost completely due to the low-velocity part of the spectrum, where the "experimental" points are consistently too low, as expected from the discretization error. This point is also clear from the "experimental" moments $\langle\langle u^\alpha \rangle\rangle$, defined as the $\langle\langle u^\alpha\,(t_R)\rangle\rangle$, but with time-integrated $N(u, t_R \mid j_c)$

$$\langle\langle u^{-1}\rangle\rangle_e = 1.218, \qquad \langle\langle u\rangle\rangle_e = 1.286, \qquad \langle\langle u^2\rangle\rangle_e = 2.031 \tag{3.7a}$$

which must be compared with the theoretical values

$$\langle\langle u^{-1}\rangle\rangle = 1.253, \qquad \langle\langle u\rangle\rangle = 1.253, \qquad \langle\langle u^2\rangle\rangle = 2.000 \tag{3.7b}$$

The discrepancies are as expected from a shortage of slow particles. In particular, the shortfall in $\langle\langle u^{-1}\rangle\rangle$ is due almost completely to the first three velocity channels.

A qualitative explanation of the convergence of the velocity spectrum for large t_R follows from the fact that the solution of the Klein–Kramers equation must approach a Chapman–Enskog solution for $\exp[-t] \ll 1$ and x outside the boundary layer.[19],[4] This solution is governed by a density in x space obeying the diffusion equation. Without absorbing boundary this density for initial velocity u_0 and initial position 0 would have the initial condition[23]

$$n(x, \tfrac{3}{2}) = \delta(x - u_0) \tag{3.8a}$$

To account, at least approximately, for the absorbing boundary we introduce an *ad hoc* correction factor $c(u_0)$ for absorption prior to $t = 3/2$ and impose the boundary condition mentioned after (2.16):

$$n(-x_M, t) = 0 \qquad (t > 3/2) \tag{3.8b}$$

The diffusion equation with this boundary condition can be solved by the method of images; the solution is

$$\begin{aligned} n(x, t) = c(u_0)[4\pi(t - 3/2)]^{-3/2}\{&\exp[-(x - u_0)^2/4(t - 3/2)] \\ &- \exp[-(x + 2x_M + u_0)^2/4(t - 3/2)]\} \end{aligned} \tag{3.9}$$

[4] For an informal survey see Ref. 22.

This implies a current, measured at $x = -x_M$, equal to

$$(4\pi)^{-1/2}(t-3/2)^{-3/2}c(u_0)(x_M+u_0)\exp[-(x_M+u_0)^2/4(t-3/2)]$$

This type of t dependence is also found for the number of particles returning to the boundary at large t_R in our simulation.

For very high t values the density profile (3.9) becomes linear over a large range of x values, and the spectrum of emerging particles should become that of the Milne solution (2.15). This limit is not quite reached in our simulation; the average velocity of the particles returning at $8 < t_R \leqslant 15$ is 97% of that in the Milne solution as obtained by Burschka and Titulaer,[12] a value confirmed in the present work. The discrepancy is due to the bending over of the density profile (3.9); this leads to a lower number of particles with high negative velocities in the Chapman–Enskog region,[19] and hence also in the boundary region. Since the curvature of $n(x, t)$ decreases only very slowly with t, the discrepancy is also expected to decrease very slowly, and the spectrum for $8 < t_R \leqslant 15$ can be assumed to be a good representation of that of all later returners. However, this implies a small, but systematic, underestimate of the average return velocity. An upper bound for this systematic error is given in the next section.

The physical reason for the independence of t_R of the velocity spectrum of particles at large t_R is that these particles have undergone almost complete thermalization during their sojourn in the interior region of the fluid, thereby losing their memory of the time of injection. If this is the relevant mechanism, then also the memory of the injection velocity should be lost. We observe indeed that the moments of $N(u, t_R \mid u')$ lose their dependence of u' for large t_R, starting at about $t_R = 6$ for the particles with low u', and even earlier for the faster ones.

4. THE MILNE SOLUTION

In our main simulation we injected 10^5 particles with a distribution over velocity proportional to $u'^2 \exp[-\frac{1}{2}u'^2]\,\Theta(u')$, corresponding to a density $\Theta(u')\,\phi_0'(u') \sim \Theta(u')u' \exp[-\frac{1}{2}u'^2]$. Of the returning particles we registered the return velocity distribution, in sampling intervals of 0.05, and several moments of the return velocity, for all t_R up to 15. These data were subsequently summed over t_R, with increased weight for the interval $8 < t_R \leqslant 15$ to account for particles that did not return, as explained in the previous section. In this way the second term in (2.15) and several of its moments are found; the calculation of the Milne solution at the wall $P^M(u, 0)$ is then elementary.

The result for $P^M(u, 0)$ is shown in Fig. 3. A noteworthy feature is that

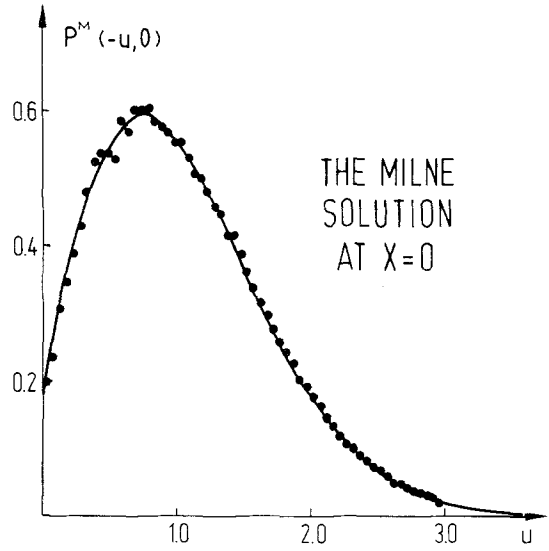

Fig. 3. The Milne solution $P^M(-u, x)$ at the wall, as determined form our simulation data. The drawn curve is the fit (4.2).

$P^M(u, 0)$ appears to approach a finite limit for $u \to 0$. However, in view of the uncertainty of the data at low u, a behavior like cu^α with $\alpha \lesssim 1/2$ cannot be excluded [the value $\alpha = 1/2$ is suggested by the asymptotic analysis[13]]. A parametrization of type (2.21) yields

$$\exp[\tfrac{1}{2}u^2]\, P^M(-u, 0) \simeq \Theta(u)[0.8415q_0(u) + 0.3681q_1(u) - 0.0602q_2(u) + 0.0271q_3(u) - 0.0132q_4(u)] \tag{4.1}$$

$$= \Theta(u)[0.1749 + 1.1286u - 0.5401u^2 + 0.1739u^3 - 0.0204u^4] \tag{4.2}$$

Adding more terms in (4.1) would not be justified; the discrepancy between the calculated $P^M(u, 0)$ and the fit (4.1) is already almost equal to the statistical uncertainty in $P^M(u, 0)$. The latter uncertainty was estimated by assigning the uncertainty $(n_i)^{1/2}$ to each number n_i of returning particles in a velocity channel (separately for $0 < t_R \leqslant 8$ and $8 < t_R \leqslant 15$) and summing their squares with the appropriate weights. According to this criterion even the significance of the coefficient of $q_4(u)$ is marginal. The results in (4.1) and Fig. 2 for not too small negative velocities are in good agreement with those in Fig. 2 of Ref. 12a.

In Table III we collect our results for several moments of $P^M(u, 0)$, foremost among them the Milne length x_M given by (2.17), as well as the corresponding results from earlier work.[12,15] The errors on our results as

Table III. Various Moments of the Distribution $uP^M(-u)$ Corresponding to the Solution of the Milne Problem

	Sim.[a]	BT[b]	Ta[b]	Tc[b]	bd1[c]	bd2[c]
$\langle\langle u^{-1}\rangle\rangle = n(0)$	0.942(8)	0.914	1.044	0.920	0.934(5)	0.985(12)
$\langle\langle u\rangle\rangle = x_M$	1.454(4)	1.461	1.440	1.485	1.464(1)	1.439(7)
$\langle\langle u^2\rangle\rangle$	2.564(17)	—	—	—	2.600(4)	2.550(22)
$\langle\langle u^3\rangle\rangle$	5.200(50)	—	—	—	5.307(11)	5.195(60)

[a] The first column is determined from our simulation with 10^5 injected particles; the statistical error is determined by comparing five subsamples of $2 \cdot 10^4$ particles.
[b] The results from ref. 12a (BT) and from two approximate calculations by the Trondheim group (ref. 15, Table III).
[c] Upper and lower bounds as derived from extreme assumptions about the systematic errors, as explained more fully in the text.

given in the first column are purely statistical errors, calculated via a separate calculation of each of the moments for five subsamples of 2×10^4 injected particles that together form our main sample. There are two sources of systematic error: the discretization of the time step and the correction for particles not returned before $t = 15$.

For the error caused by the correction for nonreturning particles we can find an upper limit. The moment $\langle\langle u^\alpha\rangle\rangle_M \equiv \langle u^{\alpha+1}\rangle/\langle u\rangle$ derived from (2.15), with $\langle u^\alpha\rangle$ indicating an average over $P^M(u, 0)$, can be written as

$$\langle\langle u^\alpha\rangle\rangle_M = \tfrac{1}{2}\langle\langle u^\alpha\rangle\rangle_c + \tfrac{1}{2}y_R\langle\langle u^\alpha\rangle\rangle_e + \tfrac{1}{2}(1 - y_R)\langle\langle u^\alpha\rangle\rangle_l \tag{4.3}$$

where $\langle\langle u^\alpha\rangle\rangle_M$ is the moment of the Milne solution, $\langle\langle u^\alpha\rangle\rangle_c$ that of $\phi_0'(u)$, $\langle\langle u^\alpha\rangle\rangle_e$ that of the contribution to $P^M(u, 0)$ from particles returning before $t = 15$, and $\langle\langle u^\alpha\rangle\rangle_l$ that of the late returners; y_R is the fraction of particles that returns before $t = 15$. The calculations in the first column of Table III were made by taking for $\langle\langle u^\alpha\rangle\rangle_l$ the results found for $8 < t_R \leqslant 15$, which probably is a slight underestimate for $\alpha \geqslant 1$, and an overestimate for $\alpha = -1$. As argued at the end of Section 3, an upper bound can be found by putting $\langle\langle u^\alpha\rangle\rangle_l$ equal to $\langle\langle u^\alpha\rangle\rangle_M$. This also results in a solvable equation for $\langle\langle u^\alpha\rangle\rangle_M$; the results so obtained for the moments are given in the next-to-last column of Table III. The difference between first and next to last columns is an upper bound, but certainly a considerable overestimate, of the systematic error due to the late returners correction.

Another estimate of the total systematic error can be deduced from the data in Fig. 2 and (3.7), the return velocity statistics for an equilibrium distribution of injected particles. Since this distribution contains many more low-velocity particles, the discretization error should be much larger for this

case and the error due to the correction for late returners somewhat smaller. Hence we obtain a *lower bound* for the $\langle\langle u^\alpha \rangle\rangle$ with $\alpha \geqslant 1$ (and an upper bound for $\alpha = -1$) when we correct the $\langle\langle u^\alpha \rangle\rangle$ found from the simulation by the factor by which the analogous result for the equilibrium distribution (3.7a) differs from the theoretical value (3.7b). The results so obtained are given in the last column of Table III. The data in the last two columns indicate that the systematic error is of the same order as the statistical one and the two sources of systematic errors work in opposite direction.

A comparison of our results in Table III with the extrapolated results of Burschka and Titulaer show excellent agreement for the Milne length and small discrepancies for the density at the wall. The latter discrepancy is not too surprising, since the extrapolation used there spanned a wide interval, and the approach of the variational estimates to the true value was so slow, that the extrapolation exponent could not be determined very precisely.[13]

The numerical result for $P^M(u, 0)$ was also expanded in the Pagani eigenfunctions using the expansion formula (2.9). This allows us to construct $P^M(u, x)$ by replacing the $\phi_n(u)$ by the corresponding $\psi_n(u, x)$ of (2.4)–(2.6). The expansion coefficients d_{+n} of (2.9c) for $P^M(u, 0)$ can be found analytically from the parametrization (4.2) and the explicit form (2.6b).[24] We determined the d^M_{+n} for $n \leqslant 12$. The contribution of $\psi_{+n}(u, x)$ to the density is also readily calculated from (2.6b); one finds

$$\begin{aligned} \int du\, \psi_{+n}(u, x) &= \exp[-xn^{1/2}](-1)^n(\pi/2n)^{1/4}(n/e)^{n/2}(n!)^{-1/2} \\ &= \exp[-xn^{1/2}](-1)^n(2n)^{-1/2}(1 - (24n)^{-1} + \cdots) \end{aligned} \tag{4.4}$$

where we used Stirling's formula.

The contribution of the first 12 boundary solutions to $n(x)$ is given in Fig. 4. This is certainly an underestimate, as is clear from the value at the wall, which has reached barely half its full value. An upper bound can also be found; the asymptotic analysis[13] shows that the d^M_{+n} have the form

$$d^M_{+n} = (-1)^n n^{-2/3} c(n^{-1/6}) \tag{4.5}$$

with $c(x)$ a smooth function decreasing with x for small enough x. The values of $c(x)$ found from the d^M_{+n} for $3 \leqslant n \leqslant 12$ are constant to within a percent; if one replaces $c(x)$ by this constant $c_0 = 0.153$ everywhere, one obtains

$$\Delta n(x) \simeq 2^{-1/2} c_0 \sum_{n=1}^{\infty} n^{-7/6} \exp[-n^{1/2}x] \equiv 2^{-1/2} c_0 Z(\tfrac{7}{6}, x) \tag{4.6}$$

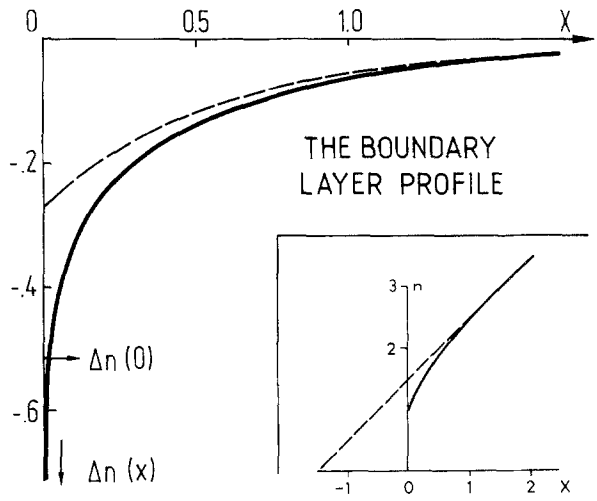

Fig. 4. The density profile in the Milne solution near the wall. The insert shows $n(x)$ and its asymptote; the main figure shows the difference $\Delta n(x)$ between the two, as approximated using the first 12 Pagani coefficients d^M_{+n} (broken curve), and from the extrapolation (4.7) (full curve). The two approximations are bounds to the actual curve; the value of the latter for $x = 0$ (obtained independently) is also shown.

The function $Z(\frac{7}{6}, x)$, which approaches $\zeta(\frac{7}{6})$ for $x \to 0$, can be calculated from the expansion (4.6) for large x and continued to smaller x via

$$Z(\tfrac{7}{6}, x) = \sum_{n=1}^{\infty} (-1)^{n+1} n^{-7/6} \exp[-n^{1/2}x] + 2^{-1/6} Z(\tfrac{7}{6}, 2^{1/2}x) \qquad (4.7)$$

The function so calculated is also shown in Fig. 4. Note its extremely fast decay for small x: between $x = 0$ and $x = 0.01$ it decreases by over 25%. This must be due to terms in (4.6) of order 10^4 and higher. This feature is shared by the exact $\Delta n(x)$.[13] The function (4.6) overestimates $\Delta n(x)$; at $x = 0$ the "overshoot" is almost 40%, but it decreases rapidly with x.

After the completion of this work a further approximate treatment of our problem, by Mayya and Sahni[26], appeared. Their results $x_M = 1.50$ and $n(0) = 0.98$ are reasonable, but especially their x_M lies outside of the bounds found in our work. They also found a steep boundary profile $n(x)$ as in our Fig. 4. A closer comparison with their work will be given elsewhere.[13]

5. THE ALBEDO KERNEL

By keeping track of the injection velocities of the particles in our main simulation sample, we could concurrently amass data on the spectrum of

return velocities of samples of particles with injection velocities in intervals of u' with a width chosen as 0.05. After correction for nonreturning particles according to (3.6) this yields a numerical determination of the albedo kernel $A(u \mid u')$. Since the main sample contains few particles with low velocities, with moreover a skewed distribution over the sampling intervals, we supplemented it for this purpose with 3000 particles distributed uniformly over the interval $0 < u' < 0.5$ (the improved sample was also used for Fig. 2).

In this section we present an analytical representation for the data so obtained for $A(u \mid u')$, or rather for

$$f_-(u \mid u') = u^{-1} A(u \mid u') \tag{5.1}$$

the density distribution at $u < 0$ for unit injected current at velocity u'. More specifically, we search for analytic functions $f_-^a(u \mid u')$ such that the representation error

$$\Delta_a = \int_0^\infty du \, |f_-(u \mid u') - f_-^a(u \mid u')|^2 \, \rho(u) \tag{5.2}$$

with an appropriate weight function $\rho(u)$, is minimal. Ideally, $\rho(u)$ should be the inverse square of the uncertainty in $f_-(u \mid u')$. Since $A(u \mid u')$ is measured as a number of particles in a given channel, its statistical uncertainty is equal to its square root; this suggests a weight

$$\rho(u) \sim u[f_-(u \mid u')]^{-1} \tag{5.3}$$

Obviously it is inconvenient to adopt separate $\rho(u)$ for each u'; since, moreover, most $f_-(u \mid u')$ are roughly of the form $(a + bu) \exp[-\frac{1}{2}u^2]$ with b much larger than a, we can attain a great analytical simplification at moderate cost in the fidelity of the fit by choosing

$$\rho(u) = \exp[\tfrac{1}{2}u^2] \tag{5.4}$$

this choice gives a somewhat too large weight to the data at low u. An orthonormal set of functions with respect to this weight function is given by

$$Q_n(u) = \exp[-\tfrac{1}{2}u^2] \, q_n(u) \tag{5.5}$$

with $q_n(u)$ the polynomials introduced in Section 2 and tabulated in Table I. The expansion formula with respect to the basis (5.5) is given by (2.21).

We found that our data for $f_-(u \mid u')$ for all u' could be fitted with a linear combination of $Q_n(u)$ with $n = 0, 1, 2, 3, 4$. The quantity Δ_a defined by (5.2) is then of the same order of magnitude as the integrated statistical

uncertainty in $f_-(u|u')$ itself; any additional terms would merely fit the fluctuations in our data.

The expansion coefficients

$$s_n(u') = \int_0^\infty du\, q_n(u) f_-(u|u') \tag{5.6}$$

turn out to be smooth functions of u', especially for not too small u'. In Table IV we give the values $s_n(u')$ for the first ten velocity channels, as obtained from our simulation, for $0 \leqslant n \leqslant 4$. For $n \geqslant 2$ and $u > 0.5$ the $s_n(u')$ do not show any significant dependence on u', and we give in the table their averages over $u' > 0.5$ with their statistical error. For $n = 0, 1$ the $s_n(u')$ can be fitted well by a function of the form

$$s_n^a(u') = q_n + b_n \exp[-2.23u'] \tag{5.7}$$

the coefficients a_n and b_n are also included in the table.

The rapid approach of the $s_n(u')$ to constant values reflects the thermalization of fastly injected particles during their passage through the fluid. The quantities $s_0(u')$ and $s_1(u')$ can be fitted with the same exponential, since

Table IV. The Expansion Coefficients s_n of the Solution $f_-(u)$ of the Albedo Problem for an Input $f_+(u')$ Corresponding to a Unit Current Confined to the Indicated Velocity Intervals, as Determined from our Simulation

u' [a]	s_0	s_1	s_2	s_3	s_4
(0.0, 0.05)	6.21	−6.74	6.37	−5.57	4.64
(0.05, 0.1)	3.98	−3.79	3.07	−2.22	1.41
(0.1, 0.15)	3.00	−2.49	1.74	−1.03	0.38
(0.15, 0.2)	2.45	−1.76	1.09	−0.53	0.07
(0.2, 0.25)	2.02	−1.19	0.63	−0.16	−0.22
(0.25, 0.3)	1.80	−0.90	0.39	−0.03	−0.17
(0.3, 0.35)	1.80	−0.90	0.41	−0.01	−0.21
(0.35, 0.4)	1.62	−0.66	0.23	−0.08	0.02
(0.4, 0.45)	1.33	−0.28	−0.02	0.21	−0.30
(0.45, 0.5)	1.35	−0.31	0.05	0.17	−0.15
a_n	0.88(1)	0.32(1)	−0.14(1)	0.06(1)	−0.03(1)
b_n	1.23(10)	−1.63(13)	—	—	—

[a] For $u' > 0.5$ the moments are well represented by $s_n(u') = a_n + b_n \exp[-2.23u']$ for $n = 0, 1$ and by constants for $n \geqslant 2$. Since the errors are lowest in the lowest velocity channels it may be advisable to subtract a multiple of the Maxwell distribution from the input $f_+(u')$, such that the new $f_+(u')$ has a zero at $u' = 0$, before applying the results from this table.

a linear combination of them yields the returning current, which equals unity irrespective of u'.

A second, probably more useful, way to represent the albedo kernel is by expressing the related kernel

$$S(u \mid u') = u^{-1} A(u \mid u') u' \tag{5.8}$$

which connects the density for $u < 0$ to that for $u > 0$ in the albedo problem:

$$f_-(u) = \int du'\, S(u \mid u') f_+(u') \tag{5.9}$$

on the basis of the functions (5.5). As we already saw, the coefficients s_n of $f_-(u \mid u')$ with $n \geqslant 5$ are not significant, so we give only the coefficients connecting the first five $Q_n(u)$. As input for this calculation we need the velocity spectrum for injected velocity distributions $(u')^\alpha \exp[-\frac{1}{2}u'^2]$ with $1 \leqslant \alpha \leqslant 5$. We calculated those from the numerically determined $A(u \mid u')$ with the following corrections:

(a) as the response to $u' \exp[-\frac{1}{2}u'^2]$, the Maxwell distribution, we took the exact Maxwell distribution, which should result due to the second law of thermodynamics, rather than the calculated response shown in Fig. 2, which is influenced rather strongly by discretization errors

(b) as the response to $u'^2 \exp[-\frac{1}{2}u'^2]$ we took the result from Section 4, thus avoiding sampling errors

(c) we replaced the velocity spectra of returning particles in each of the u' intervals with $u' > 2.5$ by the average velocity spectrum of all particles with $u' > 2.5$. As we saw before, these spectra do not show any significant u' dependence in this region; on the other hand the small numbers of particles in each of these channels would lead to large statistical errors, especially in the response to $u'^\alpha \exp[-\frac{1}{2}u'^2]$ with large α.

The resulting 5×5 matrix representing $S(u \mid u')$ is given in Table V. The last row in the table gives for each column the typical amount by which the entries in each of the columns are affected by the corrections (b) and (c). This should serve as a rough measure of the statistical uncertainties in the matrix elements. A salient feature of the matrix is the rather rapid approach toward equilibrium in the course of a single passage through the fluid. The norm of the deviation from equilibrium decreases by a factor 0.44 for the second column and by a factor less than 0.25 in the remaining ones; the sum of the eigenvalues different from unity is 0.70. Since the higher $Q_n(u')$ exhibit increasingly rapid oscillations in u', whereas the response $f_-(u \mid u')$

Table V. The Expansion Coefficients s_n of the Solution $f_-(u)$ of the Albedo Problem for Inputs $f_+(u') = Q_n(u') = \exp[-(1/2)u'^2]\, q_n(u')$

Input:	Q_0	Q_1	Q_2 [a]	Q_3 [a]	Q_4 [a]
s_0	1.0000	0.4782	0.0472	−0.0243	0.0204
s_1	0	0.3671	−0.0627	0.0318	−0.0286
s_2	0	−0.2236	0.1564	−0.1039	0.0796
s_3	0	0.1005	−0.1325	0.0963	−0.0835
s_4	0	−0.0390	0.0770	−0.0715	0.0783
$\sigma/\Delta\sigma$	—	(25)	((25))	((35))	((55))

[a] The error estimates for this column are the changes in a column element effected by smoothing out of the most dangerous statistical fluctuations; the error for the second column is calculated as in Table III.

varies only slowly with u', the contracting effect of $S(u \mid u')$ will be even more pronounced for the higher $Q_n(u')$. Therefore, one may expect that the representation of $S(u \mid u')$ in Table V will yield quite good results for the albedo problem, at least for smooth $f_+(u')$.

6. PARTIALLY ABSORBING WALLS

In this section we shall show how the result obtained for the albedo kernel can be used to solve the Milne and albedo problems for partially absorbing walls. At a partially absorbing wall the returning particles with velocity u' are not all absorbed, but have a probability $W(u \mid u')$ to be reinjected into the fluid with velocity u. For the albedo problem with an imposed external current $uf^e_+(u)$ we thus obtain the equations

$$uf_+(u) = uf^e_+(u) + \int_0^\infty du' W(u \mid u') u' f_-(u') \tag{6.1a}$$

$$uf_-(u) = \int_0^\infty du' A(u \mid u') u' f_+(u') \tag{6.1b}$$

Their solution can be written

$$uf_-(u) = [1 - A * W]^{-1} * A * uf^e_+(u) \tag{6.2}$$

where the stars denote contractions with respect to the velocity variable over the half-line $0 < u < \infty$, and the inverse is also meant in the contraction

sense. The part $f_+(u)$ of the solution of the albedo problem follows immediately from (6.1a) and (6.2).

The operator $[1 - A * W]$ is invertible whenever the absorption probability

$$\tau(u') = 1 - \int du W(u \mid u') \tag{6.3}$$

does not vanish identically for all u'. To demonstrate this we first observe that $A(u, u')$ conserves the particle current and is positive for all $u > 0$ [there is always a set of finite measure of realizations of the stochastic force $\xi(t)$ in (3.1) that leads to return velocities between u and $u + \Delta u$]. Thus, for $\tau(u)$ not identically zero, $W * A$ always decreases the current when acting on a nonnegative function; thus it acts as a contraction with respect to the norm

$$\|f\| = \int_0^\infty du\, u\, |f(u)|$$

If we further assume that $A(u \mid u')$ is bounded from below for each u uniformly in u', as is suggested by the results in Section 5, an upper bound less than unity follows for the spectrum of $A * W$, and invertibility is assured. Of course this is just the outline of a possible rigorous proof. A rigorous discussion of the special case $\tau(u) = \text{const}$, using somewhat different techniques, is given in a forthcoming paper by Beals and Protopopescu.[28] The solution of the Milne problem with partially absorbing wall can be related to the solution (6.2) just as the solution (2.15) can be related to (2.13). We shall denote this modified Milne solution by $P_M^W(u)$; it is given by

$$uP_M^W(u) = u\phi_0'(u) + [1 - A * W]^{-1} * A * [u'\phi_0'(u')\,\Theta(u')] \tag{6.4}$$

The solution $P_M^W(u)$ has a particularly simple form if the particles not absorbed at the wall are reflected diffusely:

$$W_\tau(u \mid u') = (2\pi)^{1/2} u\phi_0(u)[1 - \tau(u')] \tag{6.5}$$

Since $A(u \mid u')$ leaves $u'\phi_0(u')$ invariant, the solution $P_M^{W_\tau}(u)$ must have the form

$$P_M^{W_\tau}(u) = P^M(u) + \alpha_\tau \phi_0(u) \tag{6.6}$$

The coefficient α_τ can be determined by requiring that the particles not absorbed at the wall are all reinjected:

$$\int_{-\infty}^0 du' \,|u'|\, [1 - \tau(u')][P^M(u') + \alpha_\tau \phi_0(u')] = \int_0^\infty du\, u\alpha_\tau \phi_0(u) \tag{6.7a}$$

or

$$\alpha_\tau \int_0^\infty du\, u\tau(u)\, \phi_0(u) = \int_{-\infty}^0 du\, |u|\, [1 - \tau(u)]\, P^M(u) \tag{6.7b}$$

This formula allows an analytical evaluation of α_τ if we use the representation (4.1) for $P^M(u)$ and $\tau(u)$ is sufficiently simple. In particular, if we choose

$$\tau(u) = \Theta(|u| - u_t) \tag{6.8}$$

i.e., all particles faster than u_t are absorbed and all slower ones are reflected, then (6.7a) should reduce to Eq. (4.3) of Ref. 12b. (Unfortunately, this formula contains a misprint: the integral should be taken from $-u_t$ to 0, not form $-\infty$ to $-u_t$. The explicit calculations in Ref. 12b used the correct expression.)

The density profile $n_\tau^M(x)$ obtained from the continuation $P_M^{W_\tau}(u, x)$ of (6.6) is simply the density $n_\tau^M(x)$ shown in Fig. 4, shifted upwards by the amount $(2\pi)^{1/2}\alpha_\tau$. In particular the Milne length x_M^τ corresponding to this solution is given by

$$x_M^\tau = x_M + (2\pi)^{1/2}\alpha_\tau \tag{6.9}$$

This quantity for the choice (6.8) is exhibited as a function of u_t in Fig. 5. For some values of u_t it was calculated earlier in Ref. 12b. A comparison for

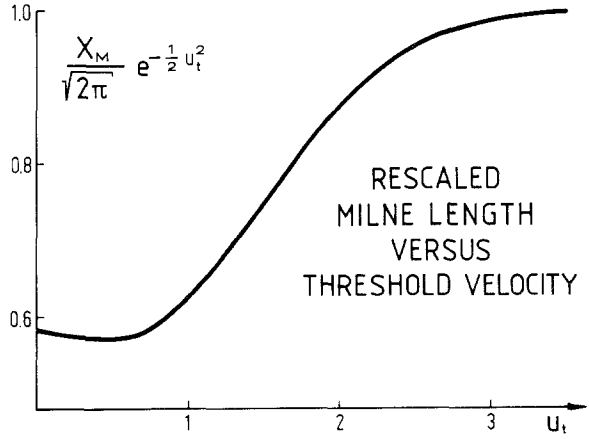

Fig. 5. The Milne length for a diffusely reflecting partially absorbing wall with sharp threshold velocity u_t, as a function of u_t. The figure shows $x_M(u_t)$ divided by the limiting expression for high threshold ("transition state theory") $(2\pi)^{1/2} \exp[(1/2)u_t^2]$.

Table VI. The Milne Length as a Function of the Threshold Velocity u_t for a Diffusely Reflecting Partially Absorbing Wall with a Sharp Absorption Threshold at u_t

u_t	0.500	0.707	1.000	1.414	2.000	4.000
$x_M(u_t)$[a]	1.617	1.871	2.589	4.966	16.20	7469
BT[b]	1.63	1.88	2.59	4.94	16.14	7468

[a] This row gives our results.
[b] This row gives the results of Ref. 12b.

these values of u_t is contained in Table VI. The agreement is excellent in spite of the shortcomings of the approximation for $P^M(u)$ employed in the earlier work.

To conclude this section we note that our results can also be used to construct the stationary boundary layer solution for a completely reflecting wall, i.e., for $\tau(u) = 0$ in (4.3). This requires finding the eigenfunction of $A * W$ with eigenvalue 1, as is evident from (6.1) with $f_+^e = 0$. A nontrivial result is found only when W does not leave the equilibrium distribution $u\phi_0(u)$ invariant. In fairness it should be pointed out that the reduction to a one-dimensional problem, as discussed in connection with (2.2), depends on the fact that three-dimensional $W(\mathbf{u} \mid \mathbf{u}')$ does not disturb thermal equilibrium in the tangential components of $\mathbf{u}'$. This severely limits the number of realistic nontrivial models.

7. CONCLUDING REMARKS

In this paper we presented a new numerical technique for solving Milne and albedo problems for the one-dimensional Klein–Kramers equation. The method requires considerably less computation time than that of Burschka and Titulaer.[10,12] We confirmed the main results of Ref. 12, especially those for the Milne length; thus we corroborate their status as a yardstick for approximate treatments,[15,17] which are simpler, but hard to assess. In a number of respects our results go beyond those of Ref. 12; we mention in particular the parametrization of the albedo kernel in Section 5 and of the velocity distribution at the wall in Section 4.

The main limitation of our treatment is that to essentially one-dimensional problems. The basic requirement is that the geometry should be planar, and that the particles *injected* into the fluid should have a Maxwell distribution with respect to their tangential velocities; in any three-dimensional problem $f_+^e(\mathbf{u})$ and $W(\mathbf{u} \mid \mathbf{u}')$ should be Maxwellian in $\mathbf{u}_{tg}$. This leaves room, e.g., for a slight generalization of the diffuse reflection model

(6.5), such that $\tau(\mathbf{u}')$ does not depend on u_x' only but, say, on the kinetic energy $\frac{1}{2}|\mathbf{u}'|^2$.

Apart from those mentioned in Section 6 we see two further types of problem to which our results could be applied. First one could consider slab geometries; the formalism for this case was essentially given by Beals[25] (This paper contains an error corrected in Ref. 11.) Such calculations might prove awkward for not too thick slabs, since one is virtually forced into expansions in terms of Pagani functions, which show very slow convergence. Secondly one might tackle time-dependent problems. The necessary modifications of the formalism are alluded to briefly in Ref. 10. We merely mention here that the statistics of return velocities resolved with respect to the return time t_R allows one to determine the Laplace transform of the time-dependent generalization of the albedo kernel, at least for values of the Laplace variable small compared to the inverse of the sampling interval $\Delta t_R = 0.5$. An extension to the Klein–Kramers equation with constant external field[10] is also possible, but it would require fresh simulations for each value of the field strength.

ACKNOWLEDGMENTS

This material is based upon work supported under a National Science Foundation Graduate Fellowship to J.V.S., who also wishes to thank Dr. Alfons Geiger for helping to make his stay in Aachen possible. Further we wish to thank Dr. Vlad Protopopescu for several helpful comments and Dr. Cor van der Mee for an enlightening review of rigorous results.

REFERENCES

1. C. Cercignani, *Theory and Application of the Boltzmann Equation* (Scott. Acad. Press, Edinburgh, 1975), Chap. VI; C. Cercignani, *Trans. Theor. Stat. Phys.* **6**:29 (1977); R. L. Bowden and W. L. Cameron, *Trans. Theor. Stat. Phys.* **8**:45 (1979); T. Ytrehus, J. J. Smolderen, and J. F. Wendt, *Phys. Fluids* **18**:1253 (1975).
2. J. J. Duderstadt and W. R. Martin, *Transport Theory* (Wiley, New York, 1979), Chap. II.
3. I. Kuščer, N. McCormick, and G. Summerfield, *Ann. Phys. (N.Y.)* **30**:411 (1965).
4. L. Waldmann and H. Vestner, *Physica* **99A**:1 (1979).
5. O. Klein, *Ark. Math. Astron. Fys.* **16**(5):1 (1922); H. A. Kramers, *Physica* **7**:284 (1940).
6. M. C. Wang and G. E. Uhlenbeck, *Rev. Mod. Phys.* **17**:323 (1945).
7. S. H. Northrup and J. T. Hynes, *J. Chem. Phys.* **68**:3203 (1978); for a recent review see D. F. Calef and J. M. Deutch, *Ann. Rev. Phys. Chem.* **34**:493 (1983).
8. M. Sitarski and J. H. Seinfeld, *J. Colloid Int. Sci.* **61**:261 (1977).
9. C. D. Pagani, *Boll. Un. Mat. Ital.* **3**(4):961 (1970).
10. M. A. Burschka and U. M. Titulaer, *Physica* **112A**:315 (1982).
11. R. Beals and V. Protopopescu, *J. Stat. Phys.* **32**:565 (1983).
12. M. A. Burschka and U. M. Titulaer, *J. Stat. Phys.* **25**:569 (1981)(a); **26**:59 (1981)(b).

13. U. M. Titulaer, to be published.
14. R. E. Marshak, *Phys. Rev.* **71**:443 (1947).
15. K. Razi Naqvi, S. Waldenstrøm, and K. J. Mork, to be published, and earlier work quoted there.
16. M. J. Lindenfeld and B. Shizgal, *Phys. Rev.* **A27**:1657 (1983).
17. S. Harris, *J. Chem. Phys.* **75**:3103 (1981), and earlier work quoted there.
18. W. Feller, *An Introduction to Probability Theory and its Applications*, Vol. 1, 3rd ed. (Wiley, New York, 1968), index entries to "first passage times" and "ruin problem."
19. U. M. Titulaer, *Physica* **91A**:321 (1978).
20. G. Birkhoff and S. MacLane, *A Survey of Modern Algebra*, revised ed. (Macmillan, New York, 1953).
21. N. G. van Kampen, *Stochastic Processes in Physics and Chemistry* (North-Holland, Amsterdam, 1981), Chap. VIII.
22. U. M. Titulaer, *Proceedings of the first Escuela Mexicana de Física Estadística*, R. Peralta-Fabi, ed. (Soc. Mex. de Física, Mexico D.F., 1983), p. 221.
23. U. M. Titulaer, *J. Chem. Phys.* **78**:1004 (1983); the result is implicit in G. E. Uhlenbeck and L. S. Ornstein, *Phys. Rev.* **36**:823 (1930).
24. I. S. Gradshteyn and I. M. Ryzhik, *Table of Integrals, Series and Products*, 4th ed. (Academic Press, New York, 1980), 3.462.1.
25. R. Beals, *J. Math. Phys.* **22**:954 (1981).
26. Y. S. Mayya and D. C. Sahni, *J. Chem. Phys.* **79**:2302 (1983); for a criticism of this paper see V. Protopopescu, R. Cole and T. Keyes, to be published.
27. R. Beals, *J. Diff. Eqs.*, to be published.
28. W. Greenberg and C. V. M. van der Mee, *Transp. Th. Stat. Phys.* **11**:155 (1983); W. Greenberg, C. V. M. van der Mee, and P. F. Zweifel, *Int. Eqs. Oper. Th.* **7**:60 (1984). These papers also contain references to earlier rigorous results.